CORE
Metadata, citation and similar papers at core.ac.uk
Provided by Explore Bristol Research

Tayong Boumda, R., Smith, R. A., & Pinfield, V. J. (2016). Acoustic characterization of void distributions across carbon-fiber composite layers. In D. E. Chimenti, & L. J. Bond (Eds.), 42nd Annual Review of Progress in Quantitative Nondestructive Evaluation: Incorporating the 6th European-American Workshop on Reliability of NDE: Volume 35 Edited by Leona. (Vol. 1706). [120008] (AIP Conference Proceedings; Vol. 1706). American Institute of Physics Inc.. DOI: 10.1063/1.4940593

Peer reviewed version

Link to published version (if available):
10.1063/1.4940593

Link to publication record in Explore Bristol Research
PDF-document

This is the accepted author manuscript (AAM). The final published version (version of record) is available online via AIP Publishing at http://dx.doi.org/10.1063/1.4940593. Please refer to any applicable terms of use of the publisher.

University of Bristol - Explore Bristol Research

General rights

This document is made available in accordance with publisher policies. Please cite only the published version using the reference above. Full terms of use are available:
http://www.bristol.ac.uk/pure/about/ebr-terms.html

Acoustic Characterization of Void Distributions Across Carbon-Fiber Composite Layers

Rostand B. Tayong[1,a)], Robert A. Smith[1,b)] and Valerie J. Pinfield[2,c)]

[1]*Department of Mechanical Engineering, University of Bristol, University walk, Bristol BS8 1TR, United Kingdom.*
[2]*Chemical Engineering Department, Loughborough University, Loughborough, Leics., LE11 3TU, United Kingdom.*

[a)]Corresponding author: rt14172@bristol.ac.uk
[b)]robert.smith@bristol.ac.uk
[c)]v.pinfield@lboro.ac.uk

Abstract. Carbon Fiber Reinforced Polymer (CFRP) composites are often used as aircraft structural components, mostly due to their superior mechanical properties. In order to improve the efficiency of these structures, it is important to detect and characterize any defects occurring during the manufacturing process, removing the need to mitigate the risk of defects through increased thicknesses of structure. Such defects include porosity, which is well-known to reduce the mechanical performance of composite structures, particularly the inter-laminar shear strength. Previous work by the authors has considered the determination of porosity distributions in a fiber-metal laminate structure [1]. This paper investigates the use of wave-propagation modeling to invert the ultrasonic response and characterize the void distribution within the plies of a CFRP structure. Finite Element (FE) simulations are used to simulate the ultrasonic response of a porous composite laminate to a typical transducer signal. This simulated response is then applied as input data to an inversion method to calculate the distribution of porosity across the layers. The inversion method is a multi-dimensional optimization utilizing an analytical model based on a normal-incidence plane-wave recursive method and appropriate mixture rules to estimate the acoustical properties of the structure, including the effects of plies and porosity. The effect of porosity is defined through an effective wave-number obtained from a scattering model description. Although a single-scattering approach is applied in this initial study, the limitations of the method in terms of the considered porous layer, percentage porosity and void radius are discussed in relation to single- and multiple-scattering methods. A comparison between the properties of the modeled structure and the void distribution obtained from the inversion is discussed. This work supports the general study of the use of ultrasound methods with inversion to characterize material properties and any defects occurring in composites structures in three dimensions. This research is part of a Fellowship in Manufacturing funded by the UK Engineering and Physical Sciences Research Council (EPSRC) aimed at underpinning the design of more efficient composite structures and reducing the environmental impact of travel.

INTRODUCTION

Fiber-reinforced polymer (FRP) composite laminates are increasingly being used to replace metallic components where their performance is a benefit. These composites comprise long fibers, with a high longitudinal stiffness and strength, embedded in a polymer resin matrix to ensure they stay aligned to the design direction. During the manufacturing of composite structures, defects can be introduced into the materials. Voids in the matrix represent one of the most serious of all the defects that can occur within an FRP material [2]. Depending on their shape and size, void inclusions can be classified as distributed porosity (a large number of micro-voids), discrete voids (individual large voids), layer porosity or delamination (large planar voids occurring at the interface between plies) [3]. It is essential for the NDT methods to measure porosity in the composite material with a good precision and the conventional method comprises an ultrasonic attenuation measurement using a through-transmission or back-wall-echo ultrasound C-scan. The obtained attenuation is a reasonable measure of the scattering due to micro-porosity and is related to the void volume fraction in the full thickness of the component. This method provides little information about the distribution of the porosity in depth, the size of the voids or the discrimination between layer and distributed porosity. It is preferable to characterize both the type of porosity and its depth distribution in order to increase the measurement accuracy and allow better informed concession decisions. Figure 1 presents an example of a 3D profile of a porosity-related

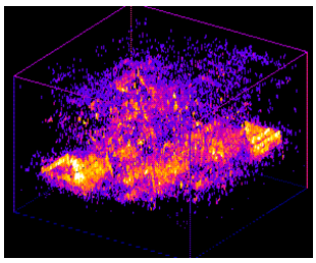

FIGURE 1. Example of a 3D profile of a porosity-related ultrasonic parameter demonstrating depth-dependence of scattering [4]. Image courtesy of QinetiQ Ltd.

ultrasonic parameter [4] illustrating some layer porosity and some distributed porosity.

The detection of porosity as well as its level is important for the NDT techniques. A wrong estimation of this defect can lead to a rejection of possible usable specimens. The nominal 'allowable' porosity threshold is between 2% and 2.5% for many composite materials in aerospace [3]. Designs must assume that this level of porosity is present and still be able to carry Design Ultimate Load, which is 1.5 times the highest load the structure will see in its entire life [5]. However, the uncertainty in a through-thickness average attenuation measurement of porosity is comparable with this allowable amount of porosity, meaning that actual porosity levels must be much lower than 2% in order to confidently pass this ultrasonic inspection test. It follows that a more accurate porosity-measurement tool, with reduced uncertainties, would allow a greater design envelope and reduce the addition of risk-mitigating weight. The following paragraph is devoted to a brief review of some state-of-art methods and studies related to this topic.

Many studies have been devoted to the estimation of porosity and they all can be classified under two main techniques: destructive and non-destructive techniques. Due to its limitations (cost and single study at a time), the former is less popular. Among these destructive techniques, there is the acid digestion method [6] which is based on gravimetry for determining the porosity content of composite materials. Non-destructive techniques are preferred as they are generally rapid, generally of low cost and allow the study of different effects such small discontinuities, internal flaws and delamination. Among these there are X-radiography [7, 8], eddy currents, shearography [7], thermography [8], acoustic emission and ultrasonic testing [7, 8]. According to Amaro et al. [7], ultrasonic methods are the best solutions for detecting the damage of composite materials. Kim et al. [9] attempted to estimate the porosity content of composite materials by applying a discrete wavelet transform to the ultrasonic pulse-echo signal. Their approach using wavelet transform relies on the decomposition of the original signal into a sum of elementary 'wavelet' contributions. This principle enables the reduction of complicated functions into several simpler ones that can be studied separately. However, in their work, the correlation between the estimated and the correct porosity is logarithmic. Their observations lead to the conclusion that the back-scattering amplitude increases with an increase of porosity. This latter result is a contradiction to the results obtained by Grolemund and Tsai [10]. Later, Feng et al. [11] suggested a micro-focus computed tomography (Micro-CT) method to examine the carbon-fiber bundles/matrix/porosity structures. Unfortunately, this method was shown to be ineffective for describing the inner behavior of the composite and a proper evaluation of the density, for example, is difficult to perform. Considering the inspection with computed tomography, Reh et al. [8] tested the use of a visualization pipeline (relying on the principle of interactive exploration and visual analysis) to examine the porosity content in CFRP specimens. Although a proper view-point of the defects was difficult to achieve, results from their work revealed the complexity of the pore shape and they definitely agreed that pore distribution, size and shape factor would have a strong influence on the ultrasonic attenuation. However, it is worth pointing out that the assumption of spherical voids used in later methods was shown to be valid for gas porosity [12]. Using a decomposition method, the work by Smith et al. [13] proposes an interesting method for decomposing the measured frequency spectrum into a series of basis functions representing porosity, thick resin layers and good structure, resulting in a coefficient for each basis function. This coefficient can then fully characterize the ultrasound response of the composite and can be used to estimate the porosity or a change of resin layer thickness or fiber-resin change [14]. Their method is shown to be effective provided porous plies are always separated by porosity-free plies. Multiple plies of porosity could not be measured correctly. In studying the porosity formation during the laser joining of CFRP and steel, Tan et al. [15] showed that the porosity has irregular shapes and the pore size ranges from tens to hundreds of microns. Very recently, Engelbart et al. [16] proposed a porosity inspection system for composite structures where no back-wall echo is obtainable. This system exhibits an interesting capability as it can indicate

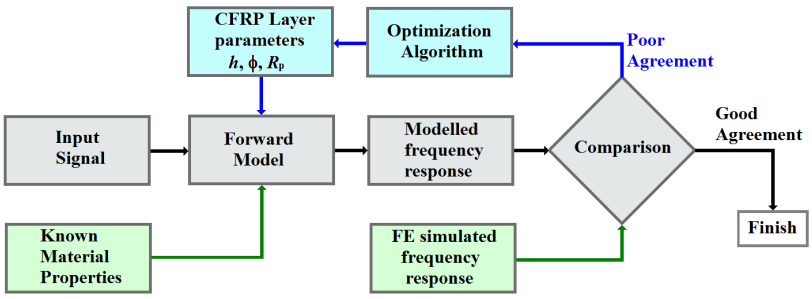

FIGURE 2. Principle of the direct and inverse modeling.

whether an additional evaluation of a certain location of the sample is needed. The method is based on a comparison of the response signal amplitude with a baseline amplitude value for a known porosity at a thickness of the location on the composite structure. Such a method is only limited to small inclined and relatively simple surfaces. Beside the frequency domain analysis, some interesting work has been carried out in the time domain. The work by Dominguez et al. [17, 18] deals with the inverse problem of determining the shape and position of obstacles embedded in an elastic medium using a topological-gradient method. In this method, the inverse problem is solved numerically using a time-reversal operator. The numerical results of the topological energy applied to various shapes of defects such as voids and cracks embedded in an aluminum slab showed relatively good results for their detection and localization. One of the advantages of the method is its robustness as noise does not seem to affect the result. However, this method requires a lengthy computation time as every position of the array needs to be computed and the whole surface of the slab has to be inspected

This paper investigates the acoustic characterization of void distributions across carbon-fiber composite layers. An attempt to address all the important features of CFRPs is made. It is assumed that layers are isotropic because the analytical model assumes normal incidence waves impinging on the specimen. The presented work is structured as follows: The next section deals with the modeling considerations where the inversion method is described as the Multi-Dimensional Optimization. Both analytical and Finite Element (FE) models are presented. This latter modeling (FE model) is only used to simulate the input data for the inversion of the properties. The following section deals with the results and discussion where the results for various scenarios of the void inclusions are depicted. The important remarks for this work are summarized in the conclusion.

THE MULTI-DIMENSIONAL OPTIMIZATION

Multi-Dimensional Optimization (MDO) finds many applications in a wide variety of problems for the detection of a local or global optimum, such as in financial modeling and statistical mechanics. In NDT methods, the searched multiple parameters represent all the system or sample properties that influence the response and are not known. A wide range of simple and more complex MDO algorithms [19] are available in the literature and the best choice depends on the number of parameters, the assumptions and constraints of the problem and the optimization criteria. In the presented work, the inversion method is built around a simulated-annealing algorithm for which the main criterion is a minimization of the error g the 'objective function', given as

$$g = \sum_i \left(y\left(\theta, \omega_i\right) - q\left(\omega_i\right)\right)^2, \tag{1}$$

where ω_i is the i^{th} angular frequency, θ is the parameter to invert, y is the analytical result and q represents the data. The solution of the optimization problem is achieved using a forward analytical model as illustrated in Fig. 2. The simulated-annealing method is a well-known algorithm developed by Kirkpatrick et al. [20] and is based on the analogy with the cooling process of a metal. It mimics the behavior of many particle systems at a finite temperature. One of its advantages is its ability to locate the global optimum avoiding the presence of other locally optimal solutions. This can be done without complicated calculations involving the first derivative of the objective function. This is of great interest for engineering problems because fast and relatively simple methods are preferred.

The inversion method described in this work focuses on calculating the layer thicknesses, void volume fraction and pore radii for a given number of stacked CFRP plies. The inversion algorithm starts by generating a random initial set of the objective parameters (initial solution). Next, a new random set of these parameters (new solution) is chosen from the neighborhood of the former solution. If the change in the objective function g is negative, the new solution is accepted to be the new current solution. Otherwise a transition step of accepting the change is computed using the Boltzmann factor $P(T)$ given as

$$P(T) = e^{-\Delta g/BT}, \tag{2}$$

where T is the current solution, B is the Boltzmann constant (usually denoted as k is the literature) and Δg is the difference or error (from the two estimates of the objective function). The Boltzmann constant simply relates the temperature to the system energy Δg. Detailed explanation of this Bolzmann constant is given in Ref.[20]. The decrease of the energy from a maximum to a minimum is regulated by a temperature representing the multi-dimensional parameter (layer thickness, porosity or pore radius). The particles can evolve to a higher or lower energy. Although there is not a clear rule on how to choose the decrement for the next solution, the work by Nolle et al. [21] suggests a factor (cooling rate) of 0.99 and an appropriate initial solution to achieve an initial transition probability of 0.5. The finalizing criterion is chosen to be when a specified minimum error value of 10^{-2} is surpassed. According to equation (2), the systems reaches a singularity at a very low temperature behavior. For this reason the cooling speed, representing the decrement rule of the algorithm, should be sufficiently slow. For this work, the initial temperature (starting point of the MDO parameter) is randomly chosen in the specific range.

MODELING CONSIDERATIONS

The multi-dimensional optimization uses an analytical forward model to predict the response of CRFPs when submitted to an ultrasound excitation. The inversion method has been tested using FE simulation to predict ultrasonic responses from various porosity distributions. In order to be consistent and applicable to porous CFRPs, the modeling should consider a number of important features: the inclusion of porosity, fiber-matrix mixture, porosity-composite mixture and the visco-elastic damping inside the layers (particularly the resin).

The Analytical Model

Various analytical methods were developed to characterize multi-layered media and the ultrasound characterization of homogeneous multi-layered systems is now relatively well understood. These methods included the transfer-matrix method as described by Hosten and Castaings [22] and the recursive compliance/stiffness matrix by Rokhlin and Wang [23]. The direct problem in this work considers a relatively simple recursive method to predict the response of CRFPs when submitted to an ultrasound excitation. In order to be consistent and applicable to porous CFRPs, the modeling should consider a number of important features: the inclusion of porosity, fiber-matrix mixture, porosity-composite mixture and the visco-elastic damping inside the layers (particularly the resin). For a plane wave propagating at normal incidence (Fig. 3) through a multi-layered material, the following expressions result from the continuity of pressure and particle velocity respectively, at any interface:

$$A_j e^{-ik_{lj}d_j} + B_j e^{ik_{lj}d_j} = A_{j+1} + B_{j+1} \tag{3}$$

$$A_j e^{-ik_{lj}d_j} - B_j e^{ik_{lj}d_j} = \frac{Z_j}{Z_{j+1}}(A_{j+1} - B_{j+1}) \tag{4}$$

where d_j, kl_j, A_j, B_j and Z_j are respectively the thickness, the longitudinal wave number, incident and reflected pressure amplitude and characteristic impedance for the j^{th} layer. Z_{j+1}, A_{j+1} and B_{j+1} are the characteristic impedance, incident and reflected pressure amplitude for the $(j+1)^{th}$ layer.

Assuming the acoustic characteristic impedance of each medium is known, the input impedance Z_{in} of n assembled layers is given by

$$Z_{in}^{(n)} = \frac{Z_{in}^{(n-1)} - iZ_n \tan(k_{lj}d_j)}{Z_n - iZ_{in}^{(n-1)} \tan(k_{lj}d_j)} Z_n, \tag{5}$$

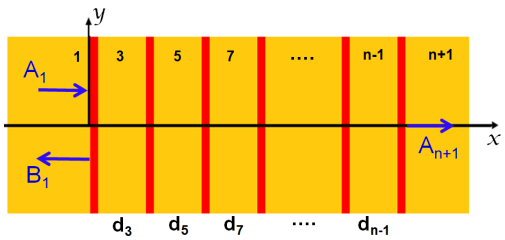

FIGURE 3. Schematic of the multi-layered material depicting the pressure amplitudes (A_1 is incident wave amplitude, B_1 is the reflected wave amplitude and A_{n+1} is the transmitted wave amplitude), layers thicknesses d_n and propagation axis. The subscript n represents the n^{th} layer. The embedding medium is denoted by subscripts 1 and $n+1$. Only normal incidence propagation along the x-axis is considered in this work.

where Z_n is the characteristic impedance of the n^{th} media, $Z_{in}^{(n-1)}$ is the input impedance considering just the first $n-1$ layers. This input impedance is calculated recursively ie. incrementing n by one each time. It is worth noticing that the input impedance of a single layer is the acoustic impedance of that layer. Assuming the acoustic impedance of the incident medium is Z_1, the acoustic pressure reflection coefficient R of the multi-layered material is obtained as

$$R = \frac{Z_{in}^{(n)} - Z_1}{Z_{in}^{(n)} + Z_1}. \tag{6}$$

One of the common methods of studying the effect of void inclusions is the use of an effective-medium approach. This method relies on replacing an inhomogeneous medium by an equivalent (also called "effective") homogeneous medium having the same acoustic behavior. The void inclusions, also called the scatterers, are known to scatter the incident wave and may disrupt the wave propagation depending on their shape and size. If λ is the excitation wavelength and r the scatterer radius, the models dealing with the scattering effect can be classified in three domains: Rayleigh (when $\lambda >> r$), stochastic (when $\lambda \approx r$) and geometric (when $\lambda << r$). The present work is focused on the Rayleigh domain. The inclusion of porosity in the analytical model is achieved using an effective-medium model based on a single-scattering approach [24, 25]. In this latter approach, multiple scattering effects are neglected and the real wave number is replaced by an effective wave number k_{eff} given as

$$k_{eff}^2 = k^2 + \frac{3\phi}{r^2} f(0), \tag{7}$$

where k is the real wave number, r is the spherical pores radius, ϕ is the void volume fraction and $f(0)$ is the backscattered amplitude for a single cavity. The basic theory of scattering from spherical voids can be attributed to Truell and his co-workers [26, 27] whose models are frequently used and extended to various voids configurations. The assumption of sphericity for the voids is shown to be valid in the case of gas porosity [12]. This effective wave number is calculated for both longitudinal and shear waves. The modeling of porous composites, particularly CFRPs, requires additional features such as accounting for the mixture of porosity with composite and fiber with matrix. In fact, the voids can either push the fibers aside or parts of the fibers can pass through the voids space. The works by Hashin [28, 29, 30] on the mixture rules for porous composite materials provide analytical solutions accounting for both the mixtures, porosity-composite and fiber-matrix. The porosity-composite mixture is accounted for following Hashin [28] for spherical isotropic inclusions and the fiber-matrix mixture is accounted for following Hashin [29, 30] for isotropic fibers in isotropic media. To account for visco-elastic damping within a layer, a complex wave number is used for which the imaginary part sets the attenuation.

The Finite Element Data Simulation

In order to develop, test and validate the inversion method, it was necessary to be able to simulate the ultrasonic response for a wide range of different parameters in the multi-layer structure. A finite-element analysis simulator was developed to achieve this. The FE results were only used to simulate the input data. For this work, the commercial FEM package Comsol Multiphysics environment was used. A 3D FE model was built for which numbers of randomly positioned voids (gaps in the model) were included, ensuring no repeating and overlapping pores. Periodic boundary conditions were set on the sides of the model. The top and bottom faces were set to absorb the incoming waves (using

'perfectly matched' layers). Continuity of pressure and velocity was ensured at the interfaces between the layers and free tetrahedral meshing with element size less than 1 μm was used. The maximum number of elements size was set to 30 per wavelength. This latter setting allowed a relatively good accuracy for the results for about 1h 45 min runtime for 64 μm x 64 μm model section and 5 layers. This reduced size of the modeled environment (compared to previous works [1]) also required a reduced size of the voids. In reality, the size of voids ranges from tens to hundreds of microns [15]. This study is focused on the determination of void volume fraction. The distribution of void sizes and their shape will be considered in terms of their influence on the accuracy of the void volume fraction measurement. For the FE model, mixture rules are considered in the porous layer following a simple volumetric approach given as

$$\Psi = \phi_g \Psi_g + (1 - \phi_g)\Psi_h, \tag{8}$$

where Ψ represents the mechanical property and the subscripts g and h are respectively used for the inclusion (fibers or voids) and the host medium. The properties used for the modeling are summarized in Table 1.

TABLE 1. Default materials properties used for the CFRP modeling. The Fiber Volume Fraction in the composite is 60%.

	Longitudinal velocity (m/s)	Shear velocity (m/s)	Density (kg/m^3)	Attenuation (dB/mm/MHz)	Thickness (μm)
Composite	2959	1870	1522	0	125
Epoxy resin	2903	1319	1270	0.15	10

Recent work [1] on this topic has attempted to show the capacity of such methods when applied to GLARE (Glass Laminated Aluminum Reinforced Epoxy). This material contains numerous highly reflective interfaces and a velocity in glass-fiber composite that is highly dependent on fiber volume fraction. The result is high-amplitude multiple reflections, narrow-bandwidth resonances and very complex pulse-echo ultrasonic responses, which vary significantly with lateral position of the probe on the surface. In [1], the analytical model is used to simulate the input data to the MDO inversion and does not consider any visco-elastic damping in the layers. The case of CFRP is significantly different to GLARE in exhibiting low reflection coefficients at inter-ply interfaces and the velocity only slightly depends on fiber volume fraction (FVF) [31]. This latter point means that no correction is required to the inverted thickness to compensate for FVF-related velocity changes. Figure 4 presents the comparison results for a CFRP specimen depicting the reflection coefficients of the analytical and the FE simulations for a single-ply between two thin resin layers (a) and a double-ply with three resin layers (b). The samples are assumed embedded into the composite medium. These spectra are the product of two frequency responses, for a single resin layer embedded in composite (a quarter-wave resonance) and the composite layer itself (a half-wave resonance). An excellent agreement throughout the frequency range is observed. For both the single ply (Fig. 4a) and the double-ply (Fig. 4b), the simulated resonant frequencies from both models are perfectly matching throughout the frequency range of study.

RESULTS AND DISCUSSION

The following subsections present the inversion of the layer thicknesses, porosities and pore radii. A composite medium is chosen as the embedding medium for the samples, rather than water, as in a recent related work [1], because the large mismatch of impedances between water and resin could affect the sensitivity to porosity. The effect of having water surrounding the sample can be investigated later. Once the FE data is collected, an artificial random noise is added to the frequency response and the resulting signal is modified by the simulated response of a 10 MHz transducer (assumed to have a Gaussian frequency response centered at 10 MHz). The width of the Gaussian frequency response is equal to the central frequency. This identical transducer response was also used in the inversion process (called the Input Signal in Fig. 2). After this modification, the resulting signal is referred to as the filtered reflection coefficient. Optimization methods are known to be sensitive to the initial guess of the parameters. In this work, the initial guess is randomly chosen in the range of [3 μm-250 μm] for the thickness, [0%-20%] for the porosity and [0 μm-5 μm] for the pore radius.

Inversion of Layer Thicknesses

Figure 5 depicts the thickness inversion results for a single CFRP ply. No porosity is considered here. In Fig.4a, the results are compared for the filtered reflection coefficient for a single ply obtained from the FE simulated data, the

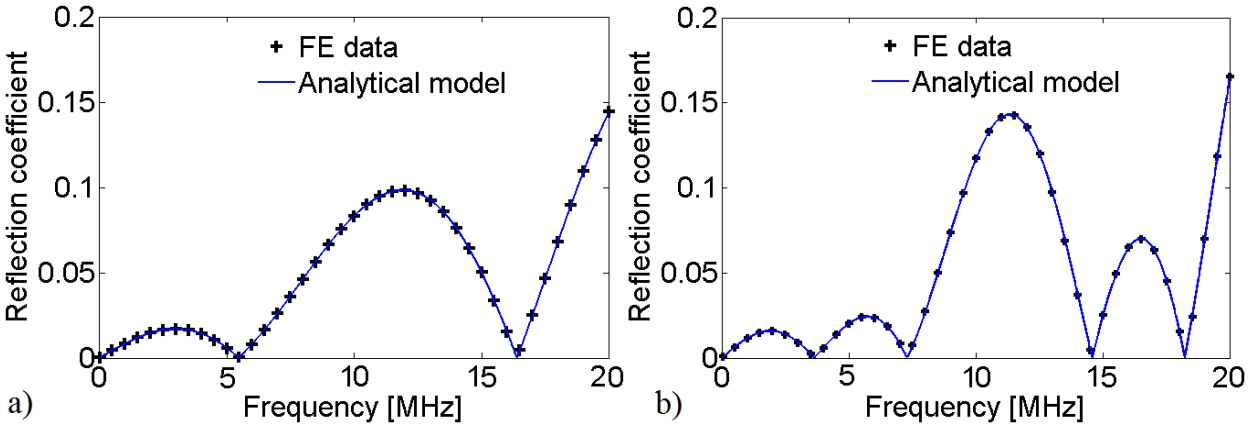

FIGURE 4. Comparison results between the analytical and the FE simulations. Reflection coefficients for a) single CFRP ply and b) double CFRP ply. The samples are assumed embedded into the composite medium.

analytical simulation with the correct values, and the analytical simulation with the inverted values (those determined using the MDO inversion algorithm). The correct and inverted values for thickness of the two resin layers (1 and 3) and the ply (layer 2) are shown in Fig. 5b.

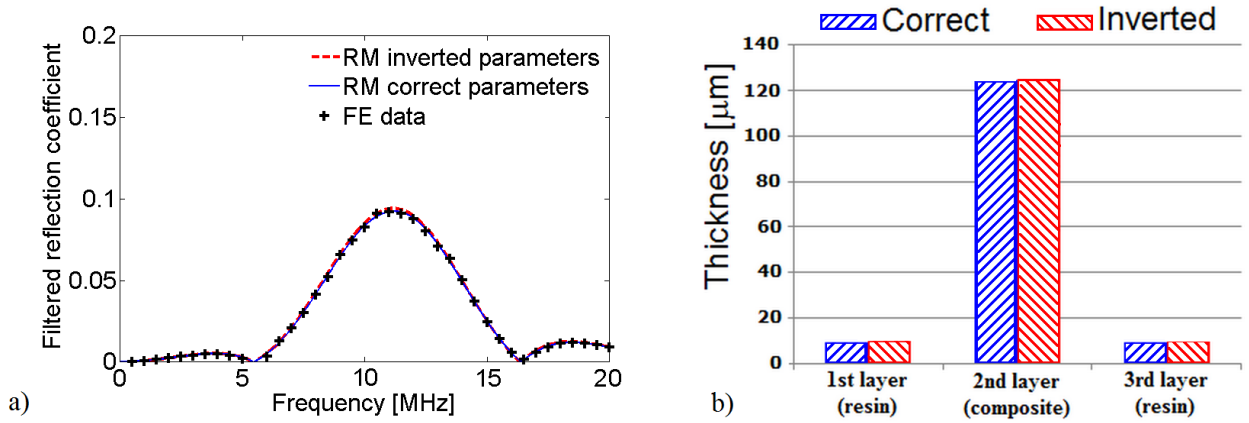

FIGURE 5. Inversion of layers thicknesses for a single CFRP ply. No porosity. a) Filtered reflection coefficient for the FE data (black curve), the Recursive Method (RM) using the correct properties (blue curve) and the RM using the inverted properties (red curve); b) Layers thicknesses correct (blue) and inverted (red) values.

Figure 6 displays the thickness inversion results for a double CFRP ply. No porosity is considered here. As for the single-ply case, a very good agreement is observed for these results. The method successfully inverts the layer thicknesses. It is worth mentioning that one of the challenges of this work is to distinguish between porosity and a change of resin layer thickness.

Inversion of Layer Porosity

Figure 7 shows the simultaneous inversion of layer thicknesses, porosity and pore radii for a double CFRP ply with 5% porosity (pore radius of 2 μm) in the 2nd resin layer only. In Fig. 7a, the filtered reflection coefficients obtained from the analytical model with the correct properties and the inverted properties both match the FE data throughout the frequency range of study. The ratio of the inverted-to-correct values of thickness, void volume fraction and pore size are shown in Fig. 7b exhibiting a very good agreement. The method was able to correctly detect the absence of porosity in the non-porous layers so this is shown as a ratio of 100%.

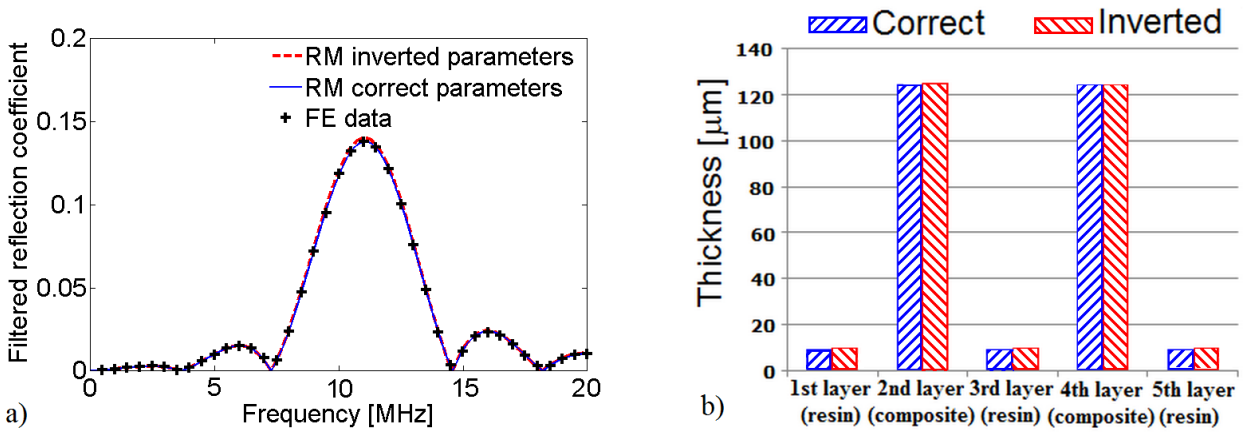

FIGURE 6. Inversion of layers thicknesses for a double-CFRP ply. No porosity. a) filtered reflection coefficient for the FE data (black curve), the Recursive method using the correct properties (blue curve) and the Recursive Method using the inverted properties (red curve); b) Layers thicknesses correct (blue) and inverted (red) values.

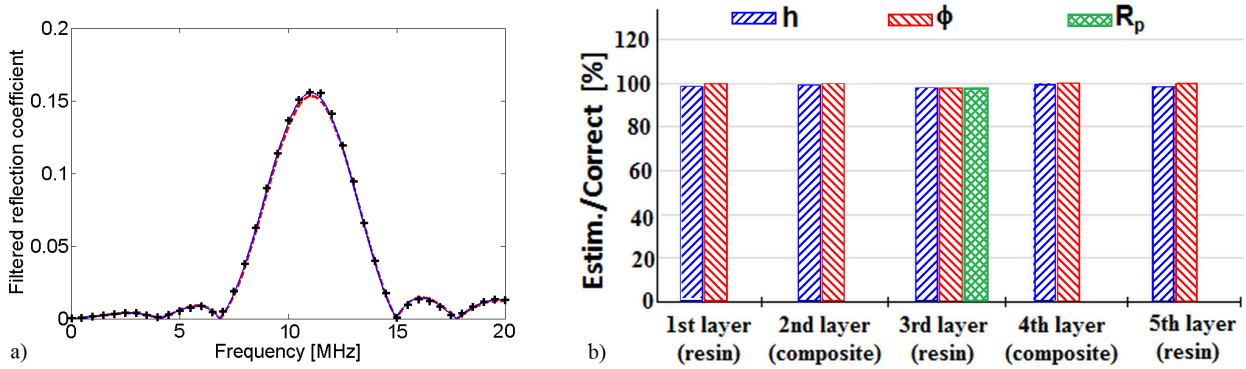

FIGURE 7. Simultaneous inversion of layers thicknesses, porosity and pores radius for a double CFRP ply. 5% Porosity located in the 2^{nd} resin layer only. Pore radius of 2 μm.

Figure 8 displays the simultaneous inversion of layer thicknesses, porosity and pore radii for a double CFRP ply. The pores are included in the first (5% porosity) and third (15% porosity) resin layers (same pore radius of 2 μm). Good agreement is observed for these results up to 13 MHz, beyond which the resonance peaks still match but the troughs exhibit different behavior in the two models. Although small errors of less than 5% were observed for the inverted void volume fraction in the resin layers, a 5% error gives void volume fraction measurements of 5.00% ±0.25% in the first resin layer and 15.00% ±0.75% in the third resin layer. In addition, the method achieved a good prediction where porosity was absent. These results strongly suggest the potential for differentiating between a change of resin-layer thickness and resin-layer porosity for relatively simple scenarios. However, a careful attention should be given to this kind of configuration as the porosity within a specific ply can shadow the effect of deeper porous plies.

Figure 9 shows the inversion for a double CFRP ply with the voids (10% porosity) included in the third resin layer only. The results for the filtered reflection coefficients are compared in Fig. 9a. Except for the troughs in the spectrum around frequencies of 14.5 MHz and 18 MHz, the analytical models with the correct and the inverted properties match the FE data well. It is worth reminding that the analytical model assumes single scattering whereas the FE model accounts for the multiple scattering. For short wavelengths, the individual pores are seen as well mixture matrix/fibre. For long wavelengths, the whole system including the pores and mixture matrix/fibre is averaged. This is considered to be one of the reasons the model would not perfectly match the FE data nodes at the high frequency range. The inversion method is able to predict no porosity in the absence of voids for both the resin and the composite layers. A good estimation for the layer thicknesses is obtained in this configuration. A small over estimation of less than 5% for the void volume fraction and 20% for the pore radii can be observed.

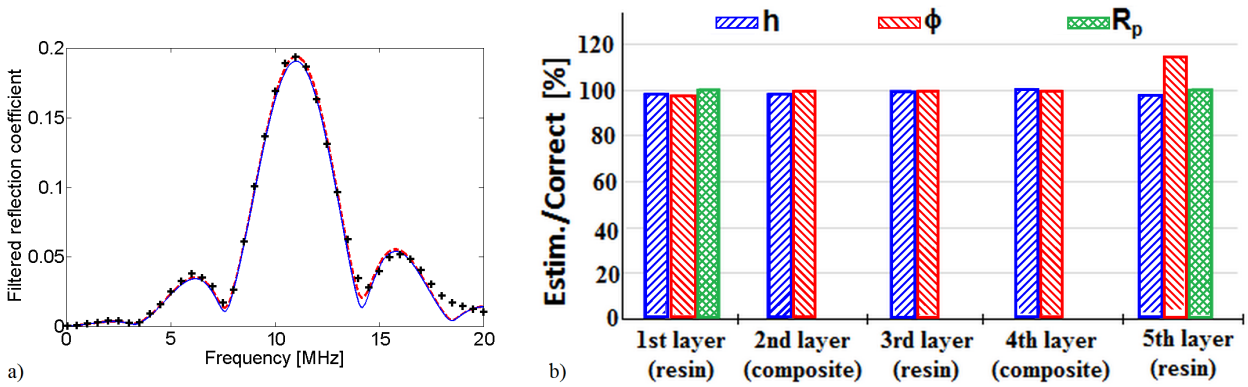

FIGURE 8. Simultaneous inversion of layers thicknesses, porosities and pores radius for a double CFRP ply. 5% and 15% porosity located in the 1^{st} and 3^{rd} resin layers. Pore radius of 2 μm.

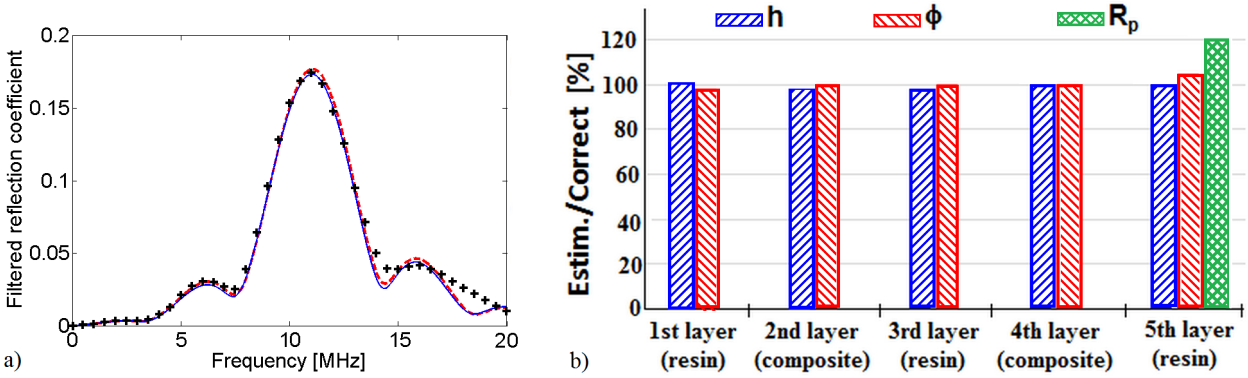

FIGURE 9. Simultaneous inversion of layers thicknesses, porosities and pores radius for a double CFRP ply. 10% porosity located in the 3^{rd} resin layers only. Pore radius of 2 μm.

CONCLUSION

For aerospace composite materials, the through-thickness average porosity level is generally estimated using ultrasound attenuation measurement in order to decide whether this defect is important or not. However, the distribution of porosity is crucially important in influencing this measurement. In certain cases, the presence of porosity in a single ply can cause more mechanical performance problems than distribution across the plies of the laminate. In this paper, an ultrasonic characterization of void distributions across carbon-fiber composite layers is described. The inversion method used multi-dimensional optimization (MDO) with an analytical forward model to calculate the sample properties. Input data was generated for testing the inversion using a Finite Element (FE) simulation. The analytical forward model predicts the response of a CRFP laminate when subjected to an ultrasonic excitation. The analytical modeling accounted for the inclusion of porosity following the single-scattering effective-medium approach of Pinfield and Challis [24, 25], the Hashin fiber-matrix mixture rule [29], Hashin [28] porosity-composite mixture rule and included visco-elastic damping in the resin. A simultaneous inversion of the thickness, porosity and pore radius in each layer showed good agreement between the inverted and correct (simulated) values for these properties. Although discrepancies of less than 5% were observed for the porosity results in the resin layers, a good agreement was still observed between the frequency-dependent filtered reflection coefficients obtained from the FE data, the analytical model with the correct properties and the analytical model with the inverted properties. Porosity was included only in the resin layers in this study, to simulate layer porosity. The inversion method could detect the lack of porosity in a layer and differentiate between thickness effects and porosity. The comparison of the forward analytical model with the FE data proved that a simple homogenized model accounting for the mixture rule and layer attenuation is capable of describing the normal-incidence frequency response resulting from the scattering of waves by the voids.

The next step for this work would be to investigate the case of porosity inside the fibrous composite ply accounting for an appropriate fiber-void-matrix mixture rule. This work suggests the potential for mapping the void volume fraction across carbon-fiber composites layers. Real data must also be considered in the next step to validate these analytical and FE models and the inversion method.

ACKNOWLEDGMENTS

This research is part of a Fellowship in Manufacturing funded by the UK Engineering and Physical Sciences Research Council (EPSRC) aimed at underpinning the design of more efficient composite structures and reducing the environmental impact of travel. Data supporting the work in this paper is freely available on application to the corresponding author.

REFERENCES

[1] I. A. Veres, R. A. Smith, and V. J. Pinfield, IEEE Trans. Ultrason. Ferroelectr. Freq. Control **62 (6)**, 1086–1094 (2015).
[2] D. E. W. Stone and B. Clarke, Non-Destructive Testing **8 (3)**, 137–145 (1975).
[3] E. A. Birt and R. A. Smith, Insight **46 (11)**, 681–686 (2004).
[4] R. A. Smith, L. J. Nelson, M. J. Mienczakowski, and R. E. Challis, Insight **51 (2)**, 82–87 (2009).
[5] E. A. S. A. Standard, "Composite aircraft structure," in *AMC 20-29* (2010).
[6] A. S. T. M. International, "Standard test method for constituent content of composite materials," in *ASTM D. 3171* (2006).
[7] A. M. Amaro, P. N. B. Reis, M. F. S. F. de Moura, and J. B. Santos, Insight **54 (1)**, 14–20 (2012).
[8] A. Reh, B. Plank, J. Kastner, E. Groller, and C. Heinzl, "Porosity maps interactive exploration and visual analysis of porosity in carbon fiber reinforced polymers," in *Proceedings of Eurographics conference on visualization (EuroVis), 31 (3), pp 1185-1194,* (2012.).
[9] K.-B. Kim, D. K. Hsu, and D. J. Barnard, NDT&E International **56**, 10–16 (2013).
[10] D. Grolemund and C. S. Tsai, IEEE Trans. Ultrason. Ferroelectr. Freq. Control **45 (2)**, 295–304 (1998).
[11] Y. Feng, Z. Feng, S. Li, W. Zhang, X. Luan, Y. Liu, L. Cheng, and L. Zhang, Composites: Part A **42**, 1645–1650 (2011).
[12] L. Adler, J. H. Rose, and C. Mobley, J. Appl. Phys. **59**, 336–347 (1986).
[13] R. A. Smith, R. E. Challis, and M. J. Mienczakwoski, "Ultrasonic composite evaluation," Tech. Rep. (Patent No WO/2010/041005, 2010).
[14] R. A. Smith, L. J. Nelson, M. J. Mienczakowski, and R. E. Challis, Insight **51 (2)**, 82–87 (2009).
[15] X. Tan, J. Zhang, J. Shan, S. Yang, and J. Ren, Composites: Part B **70**, 35–43 (2015).
[16] R. W. Engelbart, C. M. Vaccaro, S. E. Black, and N. Wood, "Porosity inspection system for composite structures with non-parallel surfaces," Tech. Rep. (Patent No 9038470, 2015).
[17] N. Dominguez, V. Gibiat, and Y. Esquerre, Wave motion **42**, 31–52 (2005).
[18] N. Dominguez, "Modelisation de la propagation ultrasonore en milieu complexe - application au controle non destructif et a la caracterisation de la porosite dans les materiaux composites stratifies," Ph.D. thesis, PhD thesis, Universite Paul Sabatier de Toulouse 2006.
[19] R. Fletcher, *Practical methods of optimization*, edited by 2nd ed. (John Wiley & Sons, New York, 1987).
[20] S. Kirkpatrick, C. D. Gelatt, and M. P. Vecchi, Science **220**, 671–680 (1983).
[21] L. Nolle, D. A. Armstrong, A. A. Hopgood, and J. A. Ware, Int. Knowledge-Based Intelligent Eng. System **6 (2)**, 104–111 (2002).
[22] B. Hosten and M. Castaings, J. Acoust. Soc. Am. **94 (3)**, 1488–1495 (1993).
[23] S. I. Rokhlin and L. Wang, International Journal of Solids and Structures **39**, 5529–5545 (2002).
[24] V. Pinfield and R. Challis, Journal of Physics: Conference Series **269**, 1742–6588 (2011).
[25] V. Pinfield and R. E. Challis, J. Acoust. Soc. Am. **129 (4)**, 1851–1856 (2011).
[26] C. F. Ying and R. Truell, J. Appl. Phys. **27**, 1086–1097 (1956).
[27] P. C. Waterman and R. Truell, J. Math. Phys. **2**, p. 512 (1961).
[28] Z. Hashin, J. Appl. Mech. **29**, 143–150 (1962).
[29] Z. Hashin, J. Mech. Phys. Solids **13**, 119–134 (1965).
[30] Z. Hashin, J. Appl. Mech. **46**, 546–550 (1979).
[31] R. A. Smith, "Use of 3d ultrasound data sets to map the localised properties of fibre-reinforced composites," Ph.D. thesis, Ph.D. thesis, University of Nottingham 2010.